J. Condensed Matter Nucl. Sci. 19 (2016) 145–154

Research Article

High-energetic Nano-cluster Plasmoid and its Soft X-ray Radiation

A. Klimov*, A. Grigorenko, A. Efimov, N. Evstigneev, O. Ryabkov, M. Sidorenko, A. Soloviev and B. Tolkunov

Limited Liability Company – New Inflow, Osenny blv. bld.6, apt.348, 121609 Moscow, Russian Federation

Abstract

Artificial stable microwave (MW) plasmoids were obtained and studied by Kapitsa in swirl gas flow. This MW plasmoid had unusual physical properties close to those of *natural ball lightning*. We studied the physical parameters and properties of a longitudinal heterogeneous plasmoid (plasma formation with erosive nano-clusters) created by capacity coupled high-frequency (HF) discharge in high-speed swirl flow in our previous papers. These nano-clusters were created by an electrode's erosion in a plasma reactor. Measurement of the power balance of this heterogeneous plasmoid is very important for aluminium–hydrogen power energetics, using a new plasma generator with high coefficient of performance (COP). This work is a continuation of our previous work. We determined that there is extra power released in heterogeneous plasmoids created by combined discharge (HF discharge + DC discharge). The measured COP in this plasmoid is about 2–10. We suppose that this extra power release in a heterogeneous plasmoid is connected with LENR. The obtained experimental results (COP, optical spectra, soft X-ray spectra, chemical composition of dusty particles) prove our suggestion. It was revealed that a heterogeneous non-equilibrium plasmoid creates intensive soft X-ray radiation (with quantum energy about 1–10 keV). We determined that excited and charged cluster particles are responsible for this soft X-ray radiation creation, to be exact. Parameters of heterogeneous non-equilibrium plasmoid (N_e, T_e, T_V, T_R and others) were measured in the experimental plasma vortex reactor (PVR). *The main goals of this work are the following:* (1) Creation of plasma-chemical vortex reactor (PVR) with high COP. (2) Obtaining of the key experimental results in this reactor for the future theoretical LENR model creation based on the PVR's operation.
 ISSN 2227-3123

Keywords: Plasmoid, plasma-chemical reactor, Soft X-ray radiation, Swirl flow

1. Experimental Setup PVR

A schematic of the experimental setup of the PVR is shown in Fig. 1. Test section (1) 60 mm diameter and 60 cm length of this reactor is manufactured from Quartz glass tube. There are tangential injection and axial injection of testing gas mixture into the swirl generator [2]. (2) So, it is possible to change the swirl flow parameter over a wide

*E-mail: klimov.anatoly@gmail.com

 ISSN 2227-3123

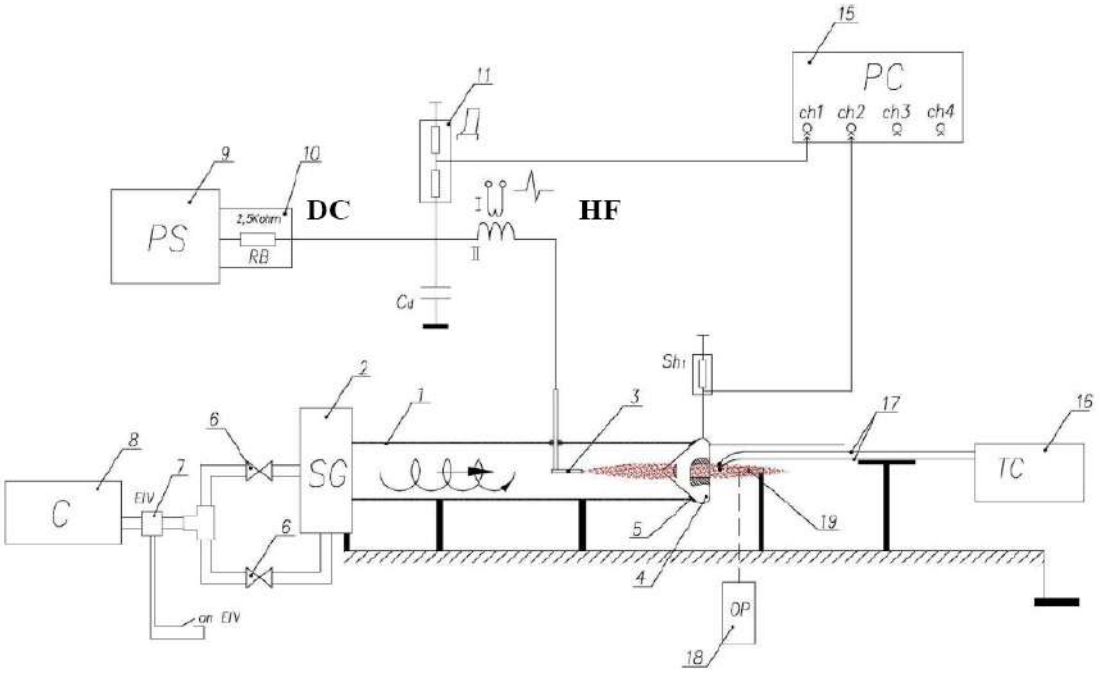

Figure 1. Schematic of experimental setup PVR. 1 – Quartz test section; 2 – swirl generator; 3 – anode; 4 – cathode- nozzle; 5 – rubber gaskets; 6,7 – valves; 8(C) – compressor, 9-PS - power supply DC, 10; 11 – high voltage probe 1:1000; 12 - current probe; 15 – oscilloscope TDS 2014B; 16,17 – thermocouples (CENTER 304); 18 – X-ray spectrometer and optical spectrometer.

range. The maximum mass flow rate is about 30 g/s in this swirl generator. The nozzle (4) is connected with PVR by rubber gaskets hermetically. Combined discharge is created in the PVR by DC power supply (PS DC) and HF power supply (HF). Mean electric power consumption used in this reactor is about 0.2–3 kW.

The following diagnostic instrumentation is used in our experiments: IR pyrometer with laser (MS6550A), thermocouple probes (CENTER 304), optical PIV device, optical spectrometer (AvaSpec 2048), X-ray spectrometer (X-123), ion mass spectrometer, high-speed video camera (Motion Pro), current probes and voltage probes, mass gas flow meter (Inflow).

The following flow and plasma parameters are measured in this work: mass flow rate of different gases (argon, water steam and others), initial gas mixture temperature, final gas mixture temperature behind the reactor nozzle, volt–ampere signals, mean electrical power input in plasma, optical spectra and X-ray spectra, high-speed video of plasmoid dynamics and discharge evolution, chemical analysis of LENR chemical species.

A heterogeneous plasmoid created by combined discharge in Ar–H_2O mixture swirl flow in the PVR is shown in Figs. 1 and 2.

2. Heterogeneous Plasmoid in Ar–H_2O Mixture Swirl Flow

Power losses in PVR are measured by electric power of nickel–chrome wire heater in pure argon flow (or known electric power consumption in argon plasma) in the beginning of each experiment (regime -PVR calibration). It was shown in the work [2–9] that there is no extra power release in pure argon flow when plasma is on.

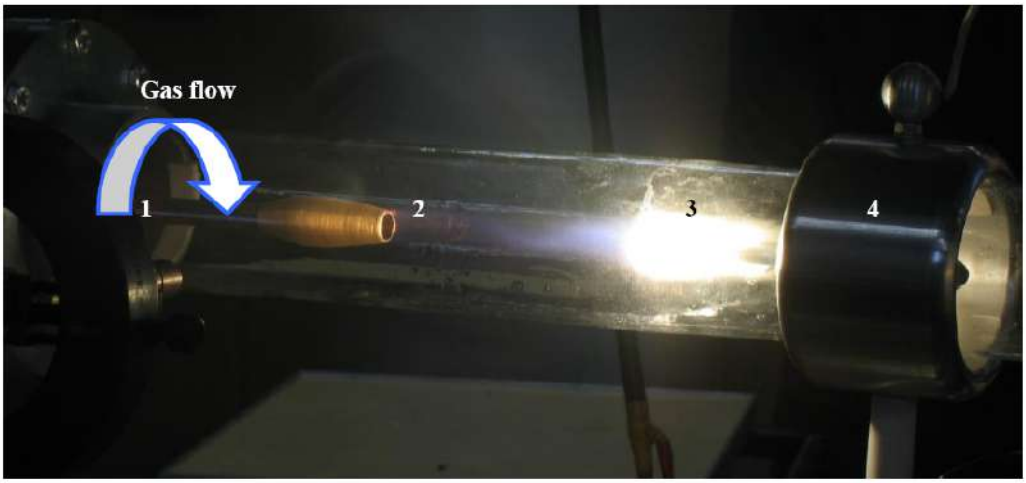

Figure 2. Heterogeneous plasmoid in PVR. 1 – swirl generator, 2 – water steam injector-anode, 3 – plasmoid near cathode and 4 – cathode.

Gas flow mixture Ar–$H_2O = 1 : 1$ is used in the experiments considered in this work. Typical images of the heterogeneous plasmoid in PVR obtained in this mixture are shown in Figs. 2 and 3. One can see that the plasmoid's length is close to the electrode's gap length of 80 mm. We determined that many tiny metal droplets are created (with diameters 0.01–0.1 mm) with plasma halos around them (diameters about of 10 mm) in the discharge zone. These metal droplets are created by hot cathode erosion. So, a large heterogeneous plasmoid consists of many small plasmoids (metal droplet kernel and plasma halo). These small plasmoids are charged formations. We measured the typical plasmoid's potential at about of $\phi \sim$ - 2–3 kV. It is important that these plasmoids can move to the anode in an external electric field at constant propagation velocity $V \sim$ 2–5 m/s (against the incoming gas flow). These droplets touch and cover the anode's surface. It is very simple to estimate electric charge and electric potential of these droplets by using of mechanic impulse equation and the Coulomb force. Note that this force equals the drag force at constant

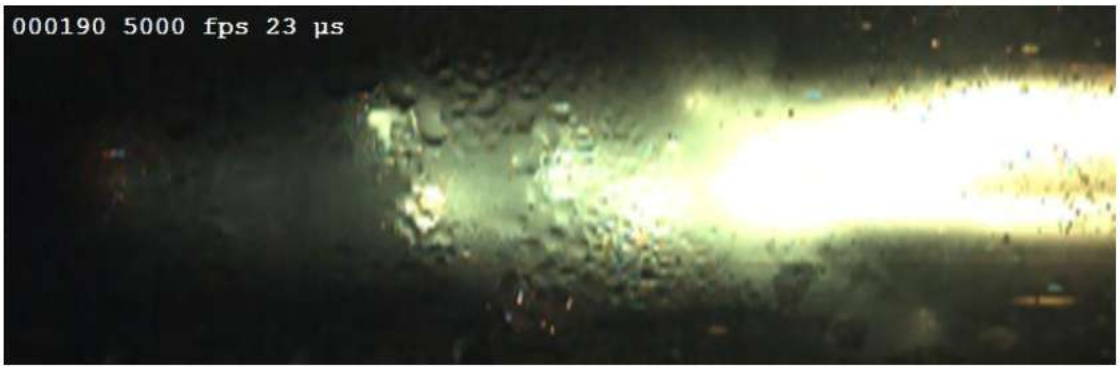

Figure 3. Frame of high-speed video. Exposure time is 20 μs. Right -cathode. Argon mass flow rate is 2 g/s and water vapour mass flow rate is 2 g/s.

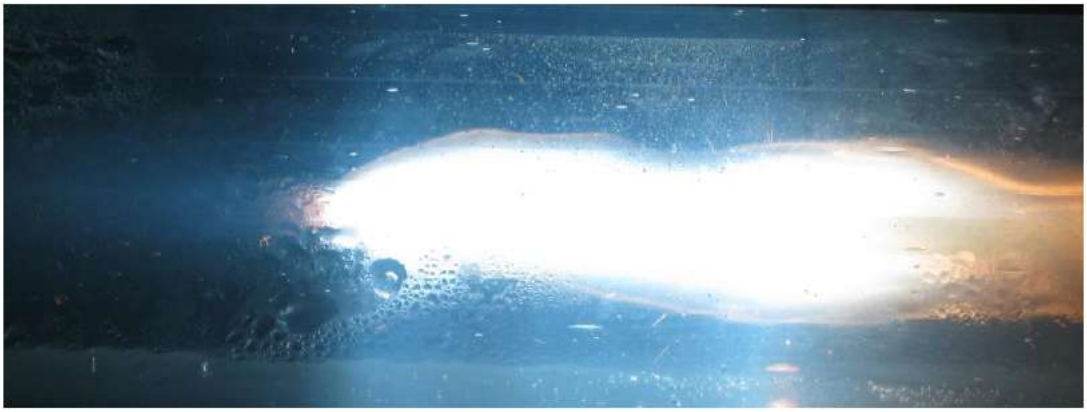

Figure 4. Integral photo of heterogeneous plasmoid 80 mm length in PVR. Exposure time 500 μs. Right -anode. Argon mass flow rate is 2 g/s and water vapour mass flow rate is 2 g/s .

propagation velocity V of these particles.

The optical spectra obtained in this experiment are shown in Figs. 4 and 5. One can see that there are the optical atomic lines Ni, H, O, Ar and the molecular band OH in these spectra. There is continuous spectrum in stable homogeneous plasmoid also, as shown in Fig. 5. This continuous spectrum is connected with hot cluster radiation (black body radiation). It is revealed that amplitudes of the hydrogen lines $I_{\alpha-\delta}$ are decreased considerably in this regime. A

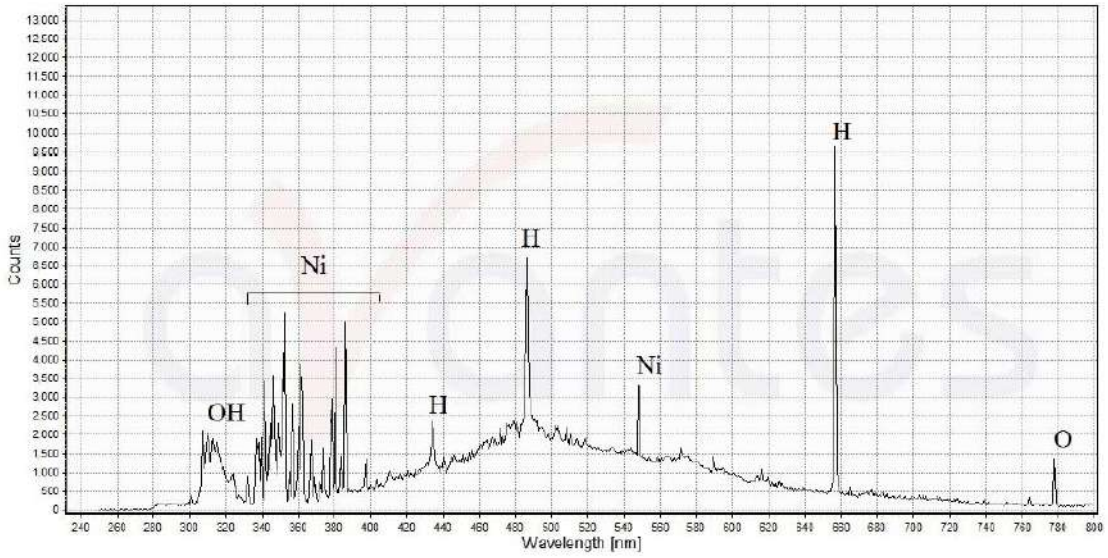

Figure 5. Optical spectrum in heterogeneous plasmoid in PVR. Starting stage of plasmoid creation. Argon mass flow rate 3 g/s, water steam mass flow rate 3 g/s .

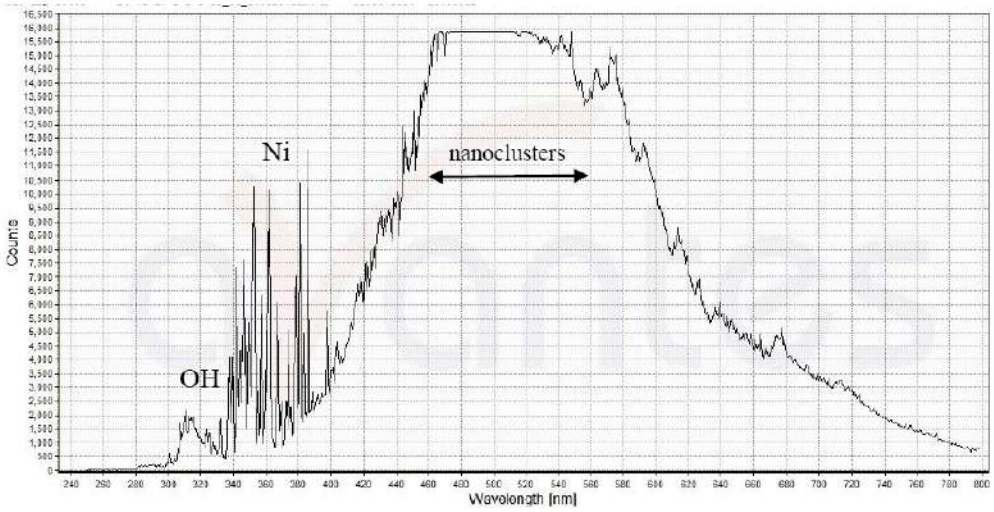

Figure 6. Optical spectrum in heterogeneous plasmoid in PVR. Final stage of plasmoid creation. Argon mass flow rate 3 g/s, water steam mass flow rate 3 g/s.

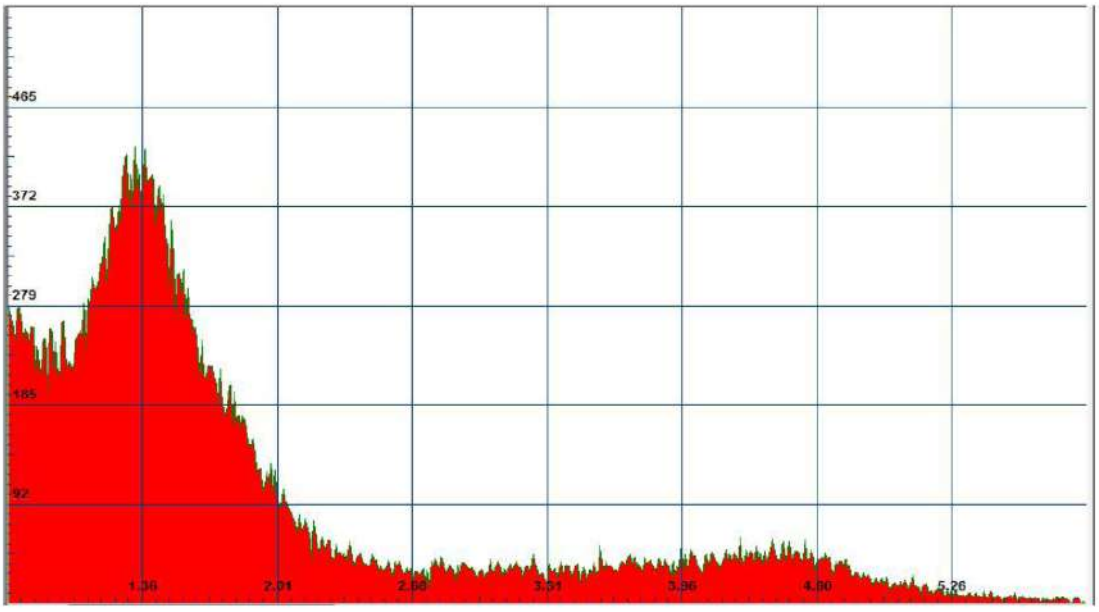

Figure 7. Soft X-ray radiation from heterogeneous plasmoid in PVR. Combined discharge (HF+DC). Power input in plasma 500 W. Mixture $Ar+H_2O = 1:1$.

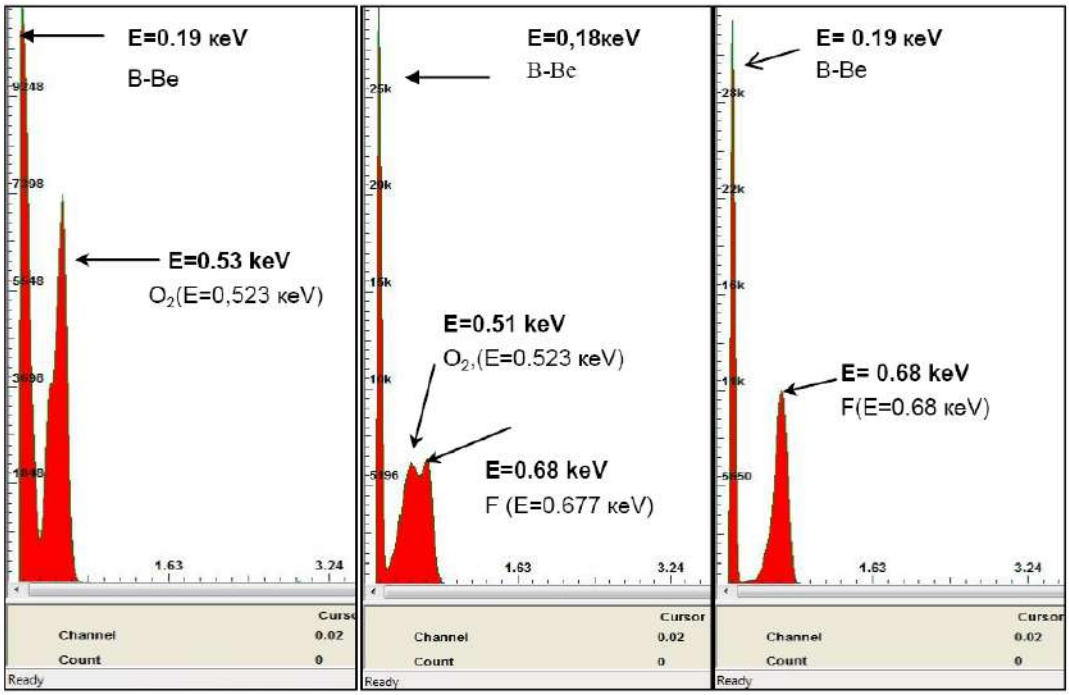

Figure 8. Soft X-ray radiation from heterogeneous plasmoid behind PVR's nozzle. X-intencity:-rel.units, quantum energy (x-axis –keV) Combined discharge (HF+DC). Power input in plasma 500 W. Mixture Ar + H_2O = 1:1. $L_b = 75$ mm- left, $L_b = 100$ mm- middle, $L_b = 120$ mm- right.

plausible hypothesis is that there is also hydrogen atom absorption by this stable heterogeneous plasmoid.

Calorimetric measurements of output gas flow behind the PVR nozzle in this plasmoid's regime are obtained. A high value COP = 6–10 is measured in this regime.

3. Soft X-ray radiation Spectra Created from Heterogeneous Plasmoid

A spectrometer (model X-123SDD) is used to record soft X-ray radiation (0.1–30 keV) from heterogeneous plasmoid. The X-ray receiver is arranged at different cross sections in PVR and behind its nozzle at L_b =1–100 cm from it. Small windows (holes) 6 mm diameters are cut in the Quartz testing section to measure X-radiation from heterogeneous plasmoids. These holes are covered by beryllium foil 40 μm thick.

Typical X-ray spectra obtained in heterogeneous plasmoid are shown in Figs. 6 and 7. One can see several peaks (maximums) in these spectra. The main peak is located near $E_1 \sim 1.3$ keV. Note that this value is close to quantum energy of $K_{\alpha 1}$ aluminum line $E_{Al} = 1.487$ keV and $E_{\alpha 1}$ magnesium line $E_{Mg} = 1.254$ keV. These chemical elements are consisting components of aluminum alloy which are used for test section manufacture. Additional peaks are located at the range E =3–5 keV. The peak E_2 = 4–4.6 keV corresponds *to the sum of resonant Ti, V, Cr lines.* These elements are consisting components of electrode material. It is impossible to explain of appearance of these lines by electron acceleration in discharge region and their interaction with metal clusters and electrodes. The measured discharge voltage is about U_d =1–2 kV only in this experiment. We determined that X-ray spectra are recorded in

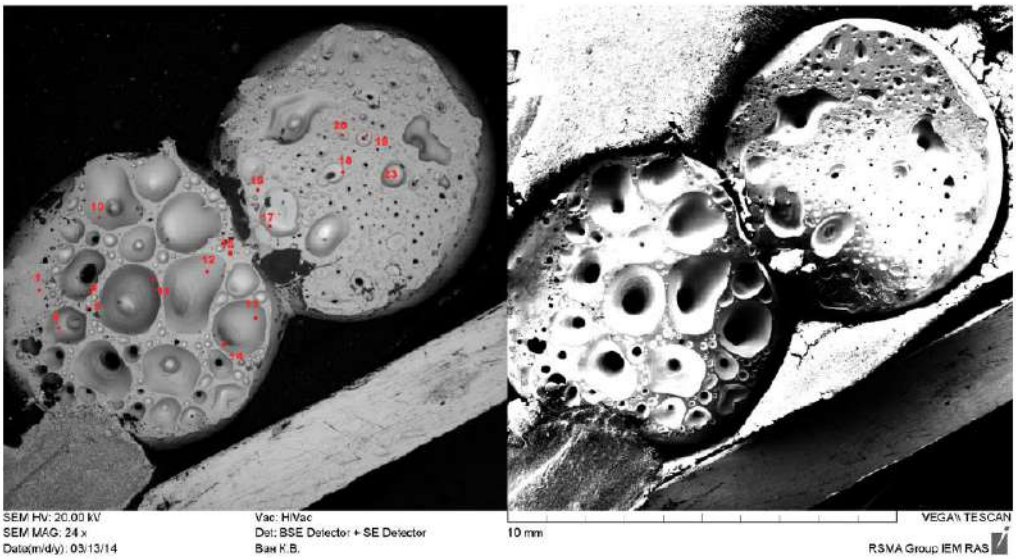

Figure 9. Melted cathode. Small holes and channels 0.1–1 mm diameter are shown in this image.

heterogeneous plasmoid, to be exact (a regime of intensive metal cluster creation in plasma). So, one can conclude that the charged and excited metal clusters can emit soft X-ray radiation.

An important result was obtained in calorimetric experiments with the PVR. We measured the maximum COP value at maximal X-radiation in this reactor. So, it is very simple to find the optimal PVR operating regime with an X-ray spectrometer.

The typical X-ray spectrum obtained behind the PVR's nozzle is shown in Fig. 7. One can see the main peaks in the range $E_1 = 0.1$–2 keV. Decay dependence of this X-ray radiation intensity on distance behind reactor's nozzle is about 30–50% at $L_\mathrm{b} \leq 1000$ mm. So, the decrement of this radiation decay is very small.

Note that the results of analysis of consequent X-ray spectra at the different cross sections L_b behind the reactor's nozzle are very interesting:

- Nitrogen line is recorded at the cross section $L_\mathrm{b} = 50$ mm,
- Oxygen line ($E_1 = 0.523$ keV) is recorded at the $L_\mathrm{b} = 75$ mm,
- F- line ($E_1 = 0.68$ keV) is recorded at the $L_\mathrm{b} = 120$ mm,
- Na, Mg, Al lines are recorded at the $L_\mathrm{b} = 150$–200 mm.

This time evolution of the X-ray spectra at the different distance L_b is clear from possible chemical element transmutation mechanism. Fluorine is absent from the surrounding air near plasma-gas jet behind the PVR nozzle. One can see splitting of the X-ray line at the $L_\mathrm{b} = 100$ mm. The first maximum is close to the oxygen line and the second one is close to the fluorine line. Then oxygen line intensity is decreased and fluorine line intensity is increased. One can see a single fluorine line at the $L_\mathrm{b} =$120–150 mm. In our opinion this element evolution may be connected with the interaction of neutron-like particles with the atmospheric chemical elements. This key result is very important for theoretical LENR model creation via PVR operation. Remember that traditional X-ray radiation is connected with electron-metal electrode interaction in strong electric fields. But the electric field is absent in regions behind the PVR's

nozzle. So, "combustion" (active reactions) of "nano-metal cluster-hydrogen fuel" continued behind the PVR nozzle. Measurement of gas flow temperature in this zone proves this suggestion. The gas temperature is increased up to 2 times at the $L_{\rm b} = 1000$ mm in our experiment comparing the one at the $L_{\rm b} = 0$.

4. Chemical Element Transmutation

Chemical analysis of exposed electrode, erosion droplets and dusty particles shows that there is chemical element transmutation connected with LENR in a heterogeneous plasmoid. A typical image of an exposed melted electrode's surface is shown in Fig. 8. One can see many thin holes (craters) on the electrode's surface. Note that crater diameter is close to the droplet's diameter. The main change of chemical composition of the electrode is located in these crater surfaces, to be exact.

Typical chemical element transmutation results are shown in Figs 9 and 10, and Table 1. These results are obtained by ion mass spectroscopy. One can see considerable change of surface electrode composition in Fig.10. There is concentration increase of the following chemical elements: sodium, aluminum, copper, chromium, manganese, magnesium, silicon and iron on the crater surfaces.

One can see that dusty particle composition is the following:- Ni ~15%, Si ~50%, Fe – 9%, Cu – 5% (see Fig. 9 and Table 1). Compare: - Ni-99.99% in the initial Ni-electrode.

The physical mechanism of chemical element transmutation was studied in detail.

Table 1. Dusty particle composition. Ion Mass spectroscopy analysis. Ni-electrodes, Gas mixture Ar: H_2O

Concentrations	Si	Ni	Fe	C	Al	Cu	Co	K	Mg
Atoms (%)	50	14,7	8,9	8,8	6,2	5,1	1,8	1,3	0,4
Molar mass (%)	31	19.2	10.9	2.3	4.7	7.2	2.4	1.1	0.2

Figure 10. Anode surface is covered by tiny metal droplets injected from cathode. Cathode diameter is 5 mm .

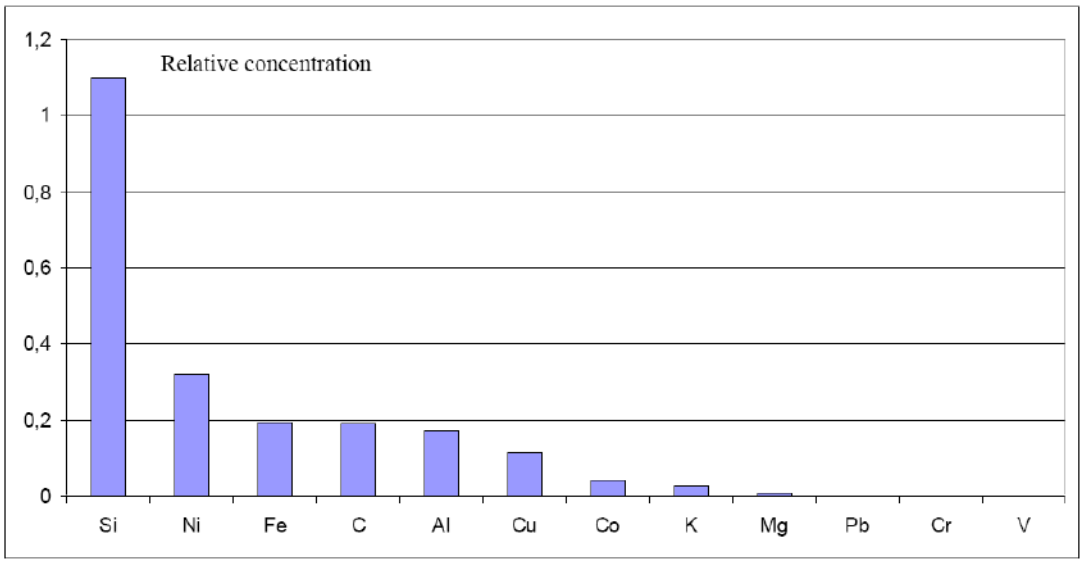

Figure 11. Relative concentrations of different chemical elements of erosive dusty particles from PVR's cathode.

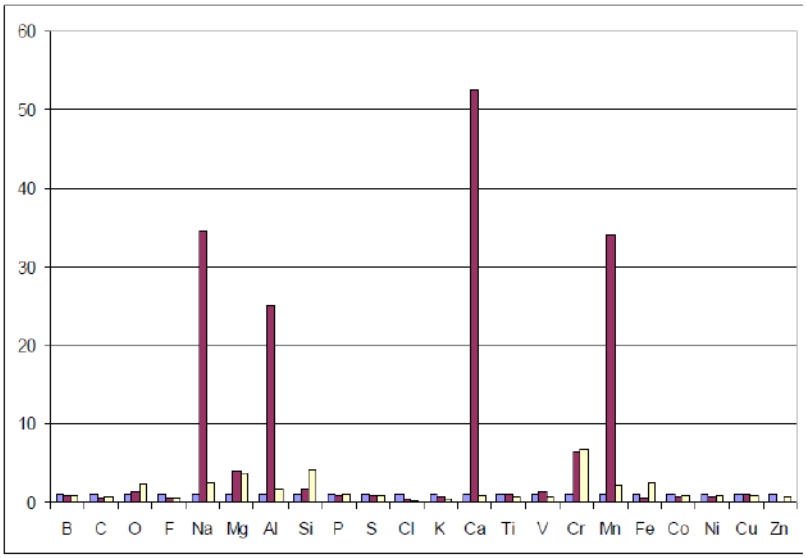

Figure 12. Relative concentrations of different chemical elements cathode's surface. All concentrations of impurities of exposed Ni-electrode are normalized on chemical element concentrations in initial Ni–electrode. Blue– initial electrode, brown– tested cathode (top side), yellow– tested cathode (lateral side).

5. Conclusions

(1) Parameters of non-equilibrium heterogeneous plasmoids in swirl flow have been measured. Electron temperature in this plasmoid is about of $T_{\rm e}$ ∼6000–7000 K. Electron concentration is about $N_{\rm e} \sim 10^{14} - 10^{15}$ cm^{-3}. Metal cluster temperature is about of $T_{\rm b} \sim 2000$ K. Rotation and gas temperatures in plasmoid less than $T_{\rm R} \sim 2300$ K. So, non-equilibrium heterogeneous plasmoids are created in the plasma vortex reactor PVR: - $T_{\rm e} \gg T_{\rm b}, T_{\rm R}$ [2–9].

(2) We determined for the first time that heterogeneous plasmoid is intensive soft X-ray radiation generator (source). The typical value of quantum energy is about of E ∼1–10 keV. We determined that the dusty plasma-gas flow behind reactor's nozzle is radioactive at long distance from it.

(3) There is chemical element transmutation in heterogeneous plasmoid. Results obtained by optical spectroscopy, ion mass spectroscopy, X-ray spectroscopy and α-ray spectroscopy prove our suggestion about transmutation.

(4) COP = 2–10 is measured in experimental setup PVR by the calorimetric method at a power release range of 1–10 kW. Estimation of specific energy release q in PVR is about 1 keV/atom. In our opinion LENR in a metal nano-cluster plasmoid may be responsible for the energy release in the PVR.

(5) We continued the Kapitsa's work [1] on stable heterogeneous plasmoid in swirl flow and proved his hypothesis about artificial ball lightning creation.

Acknowledgements

This work is supported by New Inflow, LLC. We thank Mr. V. Avdeychik, Mr. O. Grebenkin, Prof. F. Zaitsev, Prof. N. Magnitskii, for interest to this work and fruitful discussions.

References

[1] P. Kapitsa, Free plasma filament in high frequency field at high pressure, *Zhur. Exp. Teoret. Fiz.* **57**(6) (1969) 1801–1866.

[2] A. Klimov, Vortex plasmoids created by high-frequency discharges, *Atmosphere and Ionosphere: Dynamics, Processes, Monitoring,* Springer, Berlin, 2012, pp. 251–273.

[3] A. Klimov, N. Evstigneev, I. Moralev et al., Vortex control by combined electric discharge plasma, AIAA Paper 2013-1046, *51th AIAA Aerospace Sci ences Meeting*, Dallas, Texas, 2013, p.15.

[4] A. Klimov, Calorimetric measurements in vortex, *Proc. 12 Conf. CNTCE*, M. 2005, C. 246.

[5] A. Klimov, Calorimetric measurements in plasma vortex, *Proc. 14th Conf. on Cold Nuclear Transmutation and Ball Lightning*, Dagomys, 2006, pp. 246–253.

[6] A. Klimov, I. Moralev et al., Longitudinal vortex plasmoid created by capacity HF discharge, AIAA Paper 2008-956, *Proc. 46th AIAA Conf. Reno NV*, 2008, pp. 1–11.

[7] A. Klimov, V. Bityurin, I. Moralev et al., Study of a longitudinal plasmoid created by capacity coupled HF discharge in vortex airflow, AIAA Paper 2009-1046, *47th AIAA Aerospace Sciences Meeting,* Orlando, Florida, 2009, pp. 1–12.

[8] A. Klimov, Creation of new chemical elements in water by HF plasmoid, *Proc. Intern. Conf. RCCNT&BL-08*, Sochi- Dagomys, Russia, 2008, pp.15–25.

[9] A. Klimov, A. Grigorenko, A. Efimov et al., Vortex control by non-equilibrium plasma, AIAA Paper 2014, *Proc. 52nd AIAA Conf.*, 2014, pp.1–16.